1 **KCND3 potassium channel gene variant confers susceptibility to**

2 **electrocardiographic early repolarization pattern**

3 Alexander Teumer[1,2*], Teresa Trenkwalder[3*], Thorsten Kessler[3], Yalda Jamshidi[4], Marten E. van den
4 Berg[5], Bernhard Kaess[6], Christopher P. Nelson[7,8], Rachel Bastiaenen[9], Marzia De Bortoli[10],
5 Alessandra Rossini[10], Isabel Deisenhofer[3], Klaus Stark[11], Solmaz Assa[12], Peter S. Braund[7,8], Claudia
6 Cabrera[13,14,15], Anna F. Dominiczak[16], Martin Gögele[10], Leanne M. Hall[7,8], M. Arfan Ikram[5], Maryam
7 Kavousi[5], Karl J. Lackner[17,18], Lifelines Cohort Study[19], Christian Müller[20], Thomas Münzel[18,21],
8 Matthias Nauck[2,22], Sandosh Padmanabhan[16], Norbert Pfeiffer[23], Tim D. Spector[24], Andre G.
9 Uitterlinden[5], Niek Verweij[12], Uwe Völker[2,25], Helen R. Warren[13,14], Mobeen Zafar[12], Stephan B.
10 Felix[2,26], Jan A. Kors[27], Harold Snieder[28], Patricia B. Munroe[13,14], Cristian Pattaro[10], Christian
11 Fuchsberger[10], Georg Schmidt[29,30], Ilja M. Nolte[28], Heribert Schunkert[3,30], Peter Pramstaller[10], Philipp
12 S. Wild[31], Pim van der Harst[12], Bruno H. Stricker[5], Renate B. Schnabel[20], Nilesh J. Samani[7,8],
13 Christian Hengstenberg[32], Marcus Dörr[2,26], Elijah R. Behr[33], Wibke Reinhard[3]

14
15
16 1 Institute for Community Medicine, University Medicine Greifswald, Germany
17 2 DZHK (German Center for Cardiovascular Research), partner site Greifswald, Greifswald, Germany
18 3 Klinik für Herz- und Kreislauferkrankungen, Deutsches Herzzentrum München, School of Medicine,
19 Technical University of Munich, Munich, Germany
20 4 Genetics Research Centre, Institute of Molecular and Clinical Sciences, St George's University of
21 London, United Kingdom
22 5 Department of Epidemiology, Erasmus MC - University Medical Center Rotterdam, The Netherlands
23 6 Medizinische Klinik I, St. Josefs-Hospital, Wiesbaden, Germany
24 7 Department of Cardiovascular Sciences, Cardiovascular Research Centre, Leicester, Leicester,
25 United Kingdom
26 8 NIHR Leicester Biomedical Research Centre University of Leicester, Leicester, United Kingdom
27 9 Cardiology Clinial Academic Group, Institute of Molecular and Clinical Sciences, St George's,
28 University of London, United Kingdom
29 10 Institute for Biomedicine, Eurac Research, affiliated with the University of Lübeck, Bolzano, Italy
30 11 Department of Genetic Epidemiology, University Regensburg, Germany
31 12 Department of Cardiology, University of Groningen, University Medical Center Groningen, The
32 Netherlands
33 13 Clinical Pharmacology, William Harvey Research Institute, Barts and The London, Queen Mary
34 University of London, London, UK
35 14 NIHR Barts Cardiovascular Biomedical Research Centre, Barts and The London School of
36 Medicine and Dentistry, Queen Mary University of London, London, UK
37 15 Centre for Translational Bioinformatics, William Harvey Research Institute, Barts and the London
38 School of Medicine and Dentistry, Charterhouse Square, London, UK
39 16 Institute of Cardiovascular and Medical Sciences, College of Medical, Veterinary and Life Sciences,
40 University of Glasgow, Glasgow, Scotland, UK
41 17 Institute of Clinical Chemistry and Laboratory Medicine, University Medical Center of the Johannes
42 Gutenberg-University Mainz, Mainz, Germany
43 18 German Center for Cardiovascular Research (DZHK), partner site RhineMain, Mainz, Germany
44 19 The list of the Lifelines Cohort Study group authors is provided in the study acknowledgments
45 20 Department of General and Interventional Cardiology, University Heart Center Hamburg-
46 Eppendorf, Germany, DZHK (German Center for Cardiovascular Research), partner site
47 Hamburg/Kiel/Lübeck, Germany
48 21 Center for Cardiology - Cardiology I, University Medical Center of the Johannes Gutenberg-
49 University Mainz, Mainz, Germany
50 22 Institute of Clinical Chemistry and Laboratory Medicine, University Medicine Greifswald,
51 Greifswald, Germany
52 23 Department of Ophthalmology, University Medical Center of the Johannes Gutenberg-University
53 Mainz, Mainz, Germany
54 24 Department of Twin Research and Genetic Epidemiology, King's College London, London, UK
55 25 Interfaculty Institute for Genetics and Functional Genomics, University Medicine Greifswald,
56 Greifswald, Germany
57 26 Department of Internal Medicine B, University Medicine Greifswald, Greifswald, Germany
58 27 Department of Medical Informatics, Erasmus MC - University Medical Center Rotterdam, The
59 Netherlands

1

28 Department of Epidemiology, University of Groningen, University Medical Center Groningen, Groningen, The Netherlands

29 Innere Medizin I, Klinikum rechts der Isar, Technical University Munich, Munich, Germany

30 Deutsches Zentrum für Herz- und Kreislauf-Forschung (DZHK) e.V. (German Center for Cardiovascular Research), Partner Site Munich Heart Alliance, Munich, Germany

31 Preventive Cardiology and Preventive Medicine, Center for Cardiology, University Medical Center of the Johannes Gutenberg-University Mainz, Mainz, Germany; Center for Thrombosis and Hemostasis, University Medical Center of the Johannes Gutenberg-University Mainz, Mainz, Germany; DZHK (German Center for Cardiovascular Research), partner site Rhine-Main, Mainz, Germany

32 Division of Cardiology, Department of Internal Medicine II, Medical University of Vienna, Vienna, Austria

33 Cardiology Clinical Academic Group, Institute of Molecular and Clinical Sciences, St George's, University of London, United Kingdom AND St George's University Hospitals NHS Foundation Trust, London, United Kingdom

* These authors contributed equally to this work.

Corresponding Author:
PD Dr. med. Wibke Reinhard
Klinik für Herz- und Kreislauferkrankungen
Deutsches Herzzentrum München, Technische Universität München
Lazarettstrasse 36
80636 München
Germany
tel: +49 89 1218 4025
email: w.hengstenberg@dhm.mhn.de

90 **<u>Abstract</u>**

91 Background. The presence of an early repolarization pattern (ERP) on the surface electrocardiogram

92 (ECG) is associated with risk of ventricular fibrillation and sudden cardiac death. Family studies have

93 shown that ERP is a highly heritable trait but molecular genetic determinants are unknown.

94 Methods. To identify genetic susceptibility loci for ERP, we performed a GWAS and meta-analysis in

95 2,181 cases and 23,641 controls of European ancestry.

96 Results. We identified a genome-wide significant (p<5E-8) locus in the *KCND3* (potassium voltage

97 gated channel subfamily D member 3) gene that was successfully replicated in additional 1,124 cases

98 and 12,510 controls. A subsequent joint meta-analysis of the discovery and replication cohorts

99 identified rs1545300 as the lead SNP at the *KCND3* locus (OR 0.82 per minor T allele, p=7.7E-12),

100 but did not reveal additional loci. Co-localization analyses indicate causal effects of *KCND3* gene

101 expression levels on ERP in both cardiac left ventricle and tibial artery.

102 Conclusions. In this study we identified for the first time a genome-wide significant association of a

103 genetic variant with ERP. Our findings of a locus in the *KCND3* gene not only provide insights into the

104 genetic determinants but also into the pathophysiological mechanism of ERP, discovering a promising

105 candidate for functional studies.

106 Funding. For detailed information per study, see Acknowledgments.

Introduction

107
108 The early repolarization pattern (ERP) is a common ECG finding characterized by an elevation at the

109 QRS-ST junction (J-point) of at least 0.1 mV in two adjacent ECG leads. The prevalence of ERP in the

110 general population ranges from 2 to 13% being more common in young athletic men(1–5). The

111 classical notion of ERP being a benign ECG phenotype was challenged in 2008 by the landmark study

112 of Haissaguerre and colleagues showing an association of ERP with increased risk of ventricular

113 fibrillation and sudden cardiac death(6): the Early Repolarization Syndrome (ERS)(7). Since then

114 several studies demonstrated an elevated risk of cardiovascular and all-cause mortality in individuals

115 with ERP underscoring its arrhythmogenic potential(2, 8, 9). Although the mechanistic basis for

116 malignant arrhythmias in ERS is unclear, it has been suggested that they occur as a result of an

117 augmented transmural electrical dispersion of repolarization(10). Ex vivo studies point towards a

118 central role of the cardiac transient outward potassium current (I_{to}) in the development of both, ERP

119 and ERS(11). Furthermore, candidate genetic association studies have highlighted a role for several

120 genes encoding cardiac ion channels in the development of ERP and ERS(12–15). These genes

121 include gain-of-function variants in I_K-ATP channels (*KCNJ8*, *ABCC9*) and loss-of-function variants in

122 cardiac L-type calcium channels (*CACNA1C*, *CACNB2b*, *CACNA2D1*) and sodium channels (*SCN5A*,

123 *SCN10A*)(16). Interestingly, co-existence of two genetic variants in different ion channel genes with

124 opposing effects can be observed leading to phenotypic incomplete penetrance of ERP(15). However,

125 data from functional studies confirming causality are scarce(17).

126 Studies among relatives of sudden arrhythmic death syndrome show that ERP is more prevalent in the

127 relatives than in controls indicating that ERP is an important potentially inheritable pro-arrhythmic

128 trait(18, 19). Moreover, in family studies the heritability estimate for the presence of ERP was h^2=0.49

129 (20). However, estimates for common SNP heritability from unrelated individuals are lower(21). This

130 may explain why the only GWAS on ERP to date failed to identify genetic variants reaching genome-

131 wide significance(22), and indicates the need for larger GWAS with more power.

132 In order to identify genetic variations that convey susceptibility to ERP we performed a GWAS and

133 meta-analysis in European ancestry individuals, comprising 2,181 ERP cases and 23,641 controls

134 from eight cohorts that formed the discovery stage. The findings were taken forward to a replication

135 stage in 1,124 cases and 12,510 controls from four additional cohorts. To maximize statistical power

136   for locus discovery, we subsequently performed a combined discovery and replication cohort GWAS

137   meta-analysis of 3,305 ERP cases and 36,151 controls.

138   **Results**

139   Clinical characteristics of the study cohorts are depicted in **Table 1**. The proportion of ERP based on

140   the definition by Haisaguerre and Macfarlane(6, 23) ranged from 6% to 14% which is in line with

141   previously reported prevalence in the general population(2–4).

142   *Novel variants associated with ERP*

143   In the first stage, we performed a GWAS meta-analysis in up to 2,181 cases and 23,641 controls from

144   eight discovery cohorts. In total, 6,976,246 SNPs passed quality control (see Methods). We identified

145   19 variants spanning 49 kb in *KCND3* (Potassium Voltage-Gated Channel Subfamily D Member 3) as

146   well as rs139772527 (effect allele frequency [EAF] 1.4%, OR=2.57, p=2.0E-8) near *HBZ* (Hemoglobin

147   Subunit Zeta) to be genome-wide significantly associated (p<5E-8) with ERP. The SNP with the lowest

148   p-value in the region (the lead SNP) at *KCND3* was the intronic rs12090194 (EAF 32.5%, OR=0.80,

149   p=4.6E-10), and was replicated in an independent sample of 1,124 cases and 12,510 controls from

150   four additional cohorts ($p_{replication}$=2.5E-3, $p_{combined}$=9.3E-12, **Table 2**). The SNP rs139772527 near *HBZ*

151   did not fulfil the criteria for replication ($p_{replication}$=0.28, $p_{combined}$=1.4E-6, **Table 2**) as described in the

152   Methods. The subsequent combined meta-analysis of all 12 cohorts including up to 39,456 individuals

153   revealed only the locus at *KCND3* to be genome-wide significantly associated with ERP

154   (**Supplementary Figure 1**). The lead SNP of the combined GWAS meta-analysis was rs1545300

155   (EAF 31.9%, OR=0.82, p=7.7E-12), followed by the discovery stage lead SNP rs12090194 being in

156   strong linkage disequilibrium with rs1545300 (r²=0.96, D'=1) (**Figure 1**). Both SNPs were imputed at

157   very high confidence (imputation quality score >0.97) in all cohorts. The quantile-quantile plots did not

158   show any inflation (individual study λ_{GC} between 0.81 and 1.03, median: 0.91), and overall meta-

159   analysis λ_{GC}=1.02 (linkage disequilibrium [LD] score regression intercept: 1.01, see Methods)

160   (**Supplementary Figure 2**). The result of the combined GWAS meta-analysis was used for the

161   subsequent analyses. Summary statistics based conditional analysis to select independent hits did not

162   reveal any secondary signals. The association results for each stage of the lead SNPs with p<1E-6 in

163   the discovery meta-analysis are provided in **Supplementary Table 1**.

164   *Statistical finemapping of the associated locus*

165   All significantly associated SNPs of the combined GWAS meta-analysis were located within *KCND3*,

166   the potassium voltage-gated channel subfamily D member 3 gene, and were intronic (**Table 3, Figure**

167   **2**). We used these results to assess whether a single SNP or set of variants drive the association

168   signal in *KCND3* (credible set). The 99% credible set was computed based on Approximate Bayes

169   Factors for each SNP, resulting for each in a set of SNPs that with 99% posterior probability contained

170   the variant(s) driving the association signal. For the associated locus at *KCND3* the credible set

171   spanned 49 kb, and contained 19 variants. The two lead SNPs rs1545300 and rs12090194 had a

172   posterior probability of 21% and 19%, respectively, whereas the former candidate SNP

173   rs17029069(22) had a posterior probability of 2% (**Supplementary Table 2**).

174   To test whether the association in *KCND3* might be driven by heart rate or RR interval, we performed

175   a sensitivity analysis in the 1,253 ERP cases and 11,463 controls of the Lifelines cohort adjusting the

176   genetic association of rs1545300 additionally for these two traits in separate models. The effect

177   estimates were virtually unchanged (OR=0.78) with p=1.2E-7 for both adjustments. In addition, we

178   assessed whether the association of rs1545300 might be related to a specific ERP subtype i.e. ST

179   segment or ERP localization. In all subtype-stratified analyses the 95% confidence intervals of the

180   effect sizes overlapped with the overall results not pointing to a subtype driven signal (**Supplementary**

181   **Table 3**).

182   *Expression quantitative trait locus (eQTL) and co-localization*

183   We searched the Genotype-Tissue Expression (GTEx) project database(24) to look for tissue-specific

184   eQTLs including all genes in vicinity of ±1Mb of the lead SNP rs1545300 and found an association

185   with *KCND3* expression levels in tibial artery (p=3.0E-6, n=388). Two additional eQTL associations of

186   rs1545300 at FDR<0.2 across the 48 tissues tested were found with *KCND3* (ENSG00000171385.5)

187   in the left ventricle (p=2.9E-4, n=272) of the human heart, and with *CEPT1* (ENSG00000134255.9) in

188   the minor salivary gland (p=3.4E-4, n=85) (**Supplementary Table 4**).

189   Subsequent co-localization analyses of rs1545300 in these three tissues revealed also a significant

190   correlation of gene expression pattern with ERP ($p_{SMR} \leq 0.01$) (**Figure 3**, **Supplementary Table 5**),

191   where for the left ventricle the correlation seems to be attributable to the same underlying causative

192   variant ($p_{HEIDI} \geq 0.05$), and for tibial artery the test was close to nominal significance ($p_{HEIDI}=0.05$).

193   However, the significant $p_{HEIDI}=1.7E-3$ of *CEPT1* in the minor salivary gland points rather towards a

194   pleiotropic effect of rs1545300 than to a causal effect of gene expression on ERP in this tissue. For all

195   three tissues, an increased gene expression level was associated with a higher risk of ERP

196   (**Supplementary Table 5**).

197   *Pleiotropic effects of the lead SNPs*

198   To assess pleiotropic effects of the *KCND3* lead SNP rs1545300 or its proxies (r²>0.8), we looked for

199   genome-wide significant associations in the NHGRI-EBI Catalog of published genome-wide

200   association studies(25) (accessed: 07/30/2019). Pleiotropic associations were found for P-wave

201   terminal force (rs12090194 and rs4839185)(26) and for reduced risk of atrial fibrillation per minor allele

202   (rs1545300 and rs1443926)(27, 28). All these SNPs were in strong linkage disequilibrium (r²>0.97)

203   with the lead SNP. In addition, variants in low to moderate LD with rs1545300 were associated with P-

204   wave duration (rs2798334, r²=0.26)(29) and ST-T-wave amplitudes (rs12145374, r²=0.60)(30). A

205   phenome-wide lookup of rs1545300 in the association results of 778 traits available via the Gene

206   ATLAS web portal (31) using 452,264 individuals of the UK Biobank cohort revealed an association of

207   the ERP risk reducing minor T allele with reduced risk of heart arrhythmia (estimated OR=0.92,

208   p=3.6E-6). Of note, no other of the assessed traits reached significance after Bonferroni correction

209   (p<0.05/778=6.4E-5).

210   **Discussion**

211   In this GWAS meta-analysis comprising 3,305 cases and 36,151 controls including independent

212   replication samples, we describe an association of ERP with a locus on chromosome 1 in the *KCND3*

213   gene. This is the first study identifying a robust genome-wide significant association between genetic

214   variants and ERP. Our findings provide a candidate gene for further functional studies examining the

215   pathophysiological mechanism of ERP and potentially ERS. The *KCND3* gene encodes the main

216   pore-forming alpha subunit of the voltage-gated rapidly inactivating A-type potassium channel. In the

217   cardiac ventricle *KCND3* contributes to the fast cardiac transient outward potassium current (I_{to}), which

218   plays a major role in the early repolarization phase 1 of the cardiac action potential (AP).

219   To date, two competing theories explain the presence of J waves and ERP: the repolarization and the

220   depolarization theory, both involving the I_{to} channel. On the basis of animal models evidence for the

221   former is more compelling. Thus, J waves result from a transmural voltage gradient created by a more

222   prominent epicardial phase 1 AP notch relative to the endocardial AP notch(11, 32). The I_{to} current

223   notably influences the degree of the transmural heterogeneity of the phase 1 AP notch and

224 consecutively the magnitude of the J wave(11, 32). Pharmacological inhibition of the I_{to} current with 4-

225 aminopyridine results in a reduction of the J wave amplitude(11). The depolarization theory is based

226 on clinical overlap of ERP with Brugada syndrome, which has led to the suggestion of Brugada

227 syndrome being a right ventricular variant of the ERP(33). In theory, deviation from the sequential

228 activation of cardiac currents I_{Na}, I_{to}, and I_{CaL} can lead to regional conduction slowing and appearance

229 of inferior and/or lateral ERP(32, 34). In patients with ERS, distinct phenotypes of both delayed

230 depolarization and early repolarization have been identified(35).

231 ERP is a highly heritable trait within families(3, 20), however limited heritability can be attributed to

232 common SNPs in unrelated individuals(21). This might be a reason why the only GWAS to date which

233 included 452 cases failed to replicate any genome-wide significant loci(22). In our study, which

234 includes 3,334 cases, we discovered and replicated variants in the *KCND3* gene. Interestingly, one of

235 these variants (rs17029069), which is in moderate LD (r²=0.18, D'=-1) with our lead SNP rs1545300

236 (**Supplementary Figure 3**) was reported as a candidate in the earlier GWAS meta-analysis(22).

237 However, this variant did not replicate in their study, which the authors attributed to limited power

238 based on the small sample size and/or heterogeneous phenotyping. In our study, experienced

239 cardiologists evaluated more than 39,000 ECGs with high reproducibility ensuring a very high

240 phenotyping quality(21). The resulting homogenously assessed phenotype and the substantially

241 increased number of cases are two aspects that elevated the statistical power of our GWAS meta-

242 analysis. All detected variants cluster in intronic regions of the *KCND3* gene, without significant allelic

243 heterogeneity. The annotation of the locus does not point to a direct pathogenic effect, i.e. a protein

244 altering mutation, and also the statistical finemapping revealed no single SNP with a substantial

245 posterior probability (e.g. >80%) of being causal. However, the latter approach has limitations of

246 detecting rare causal variants due to imputation uncertainty and minimum minor allele frequency

247 (MAF). Nevertheless, eQTL analysis suggested that the detected variants may affect gene expression

248 of *KCND3*. Potential mechanisms include modification of gene expression via altered binding of

249 transcription factors at *cis*-elements through enhancers or in DNaseI hypersensitivity regions (**Figure**

250 **2**). This is supported by the results of the test for co-localization showing an increase of ERP risk due

251 to increased gene expression levels of *KCND3* in tissues of the human heart and tibial artery. Similar,

252 pharmacological ex vivo data predict gain of function mutations in the I_{to} current to increase the overall

253 transmural outward shift, leading to an increased epicardial AP notch and thereby inducing ERP in the

254 surface ECG(32). Additionally, in close proximity to the lead SNP rs1545300 a long non-coding RNA

255 (lncRNA), KCND3 antisense RNA 1 (*KCND3-AS1*) is described. LncRNAs have been shown to

256 physiologically influence gene regulation through various mechanism e.g. chromatin remodeling,

257 control of transcription initiation and post-transcriptional processing(36, 37). On the other hand,

258 dysregulation of lncRNA control circuits can potentially impact development of disease(38): a very

259 prominent example in cardiovascular diseases is the lncRNA *ANRIL*, which is a key effector of *9p21* in

260 atherosclerotic risk and cardiovascular events(38–40).

261 Given the high prevalence of ERP in the general population and a high MAF of the identified genetic

262 variants in our study the key question remains why only a very small subset of individuals develops

263 severe ventricular arrhythmias and ERS. The fine interplay of a genetic predisposition and specific

264 precipitating conditions might lead to an electrically vulnerable cardiac state. Insights into the potential

265 origin of ventricular arrhythmias in ERS come from animal models and highlight the role of different ion

266 channels including I_{to}(10). A pharmacological model of ERS in canine wedges from the inferior and

267 lateral ventricular wall showed marked regional dispersion of repolarization (loss of phase 2 AP dome

268 and AP shortening in some epicardial regions but not others). Presence of transmural repolarization

269 heterogeneity allowed local re-excitation in form of closely coupled extrasystolic activity (phase 2 re-

270 entry). The combination of an arrhythmogenic substrate, represented by regional electrical instability,

271 and triggering premature ventricular beats resulted in ventricular fibrillation(10). Human data in ERS

272 patients suggest that in a subgroup, the ERP is due to a pure repolarization phenotype and

273 arrhythmia(35) is triggered by Purkinje fiber ectopic beats.

274 Genetic variants in various ion channel genes have been associated with ERS(16) including the

275 *KCNJ8* and *ABCC9* genes encoding the Kir6.1 and ATP-sensing subunits of the K_{ATP} channel(6, 12,

276 41, 42). The commonly implicated variant KCNJ8-p.S422L has a population frequency not consistent

277 with ERS, and is predicted to be benign by multiple in silico algorithms according to the ClinVar

278 database(43). A recent study by Chauveau *et al.* has, however, identified a de novo duplication of the

279 *KCND3* gene in a patient who survived sudden cardiac death and in his 2-year-old daughter(13). Both

280 exhibited marked ERP in the inferolateral leads that was augmented by bradycardia and pauses in

281 heart rhythm, in keeping with a repolarization mechanism underlying the ERS phenotype. Studies

282 have suggested that the inferior region of the left ventricle has a higher density of *KCND3* expression

283 and higher intrinsic levels of I_{to}(10). This may explain the higher vulnerability of this region for the

284   development of ERS in the setting of a genetically mediated gain-of-function in the I_{to} current.

285   Moreover, observational studies also identified different ERP subtypes including the occurrence of

286   ERP in the inferior region and a horizontal/descending ST segment morphology to be associated with

287   a higher risk of sudden arrhythmic death and cardiovascular mortality(2, 44, 45). However, in a

288   subgroup of our study the association signal of ERP risk and *KCND3* variation was not dominated by a

289   specific ERP high-risk subtype. Of note the formation of subgroups led to reduction in sample size and

290   thus statistical power.

291   Taken together, the rare occurrence of ERS may be explained by different conditions. On the one

292   hand, an underlying monogenic mutation may be found in some cases. On the other, no single causal

293   mutation can be identified in the majority of ERS cases rendering the influence of multiple genes and

294   environmental factors more likely i.e. a 'multi-hit condition'. Similar to other polygenic diseases, the

295   sum of multiple minor effects of several common genetic variations together with specific external

296   triggers may affect the occurrence of ERS. There is indeed evidence to suggest that common variants

297   in the *KCND3* locus increase arrhythmogenicity. A phenome-wide lookup of our common lead SNP in

298   more than 450,000 individuals from the UK Biobank linked the minor T allele associated with reduced

299   ERP to a reduced risk of heart arrhythmia(31). Furthermore, additional data show an association of

300   the same common variant with reduced risk of atrial fibrillation(27, 28). A small effect of a common

301   SNP at *KCND3* does not necessarily mean that the variant is benign; rather a single risk allele is

302   associated with a small but effective change in the gene expression level. Thus, the overall effects of

303   the *KCND3* gene expression levels on the phenotype may appear much stronger compared to the

304   small effect of rs1545300. Based on our results, it could be hypothesized that variation in *KCND3*

305   gene expression levels and subsequently its encoded protein may affect the risk of ERP and

306   eventually ERS. The positive effect direction of the change in *KCND3* gene expression levels in heart

307   tissue on the risk of ERP estimated via the SMR test (**Supplementary Table 5**) suggests an elevated

308   risk with increasing abundance of the *KCND3* encoded protein. Functional validation is necessary to

309   validate this hypothesis and analyses of the *KCND3* gene in individuals with ERS is warranted to

310   confirm the role of *KCND3* variation in arrhythmogenesis.

311   Our study has some limitations, which need to be acknowledged. Presence of ERP in the ECG can be

312   variable, as it has been described to be dependent on age, heart rate, vagal activity and medication,

313   although our findings were valid after adjusting for some of these factors. Therefore, we cannot

314   exclude that we have missed some individuals with ERP. Second, the tissue-specific gene expression

315   data used for the co-localization analysis is based on a limited sample size. A larger gene expression

316   sample or functional studies are needed to validate the revealed effect of *KCND3* expression on the

317   ERP. Also, we analyzed only common and low-frequency SNPs with a MAF >1% missing rare variants

318   and variants not included in the imputation panel. Finally, long-term outcome data identifying those

319   individuals with ERP who suffer from ERS are not available. Further GWAS in large international

320   collaborative cohorts of ERS patients are therefore necessary to determine the genetic risk.

321   In conclusion, we show for the first time, a robust association of genetic variants with the ERP in a

322   large GWAS of individuals of European ancestry. The locus in the *KCND3* ion channel gene is an

323   intuitive candidate and supports the theory that at least a proportion of ERS is a pure channelopathy.

324   Intensive future research will be needed to extend the discovery of ERP susceptibility loci to

325   individuals of non-European ancestry, and to improve identification and risk stratification of the subset

326   of individuals with the ERP who are at highest risk for potentially lethal ventricular arrhythmias.

327   **Methods**

328   *Study cohorts and SNP genotyping*

329   The discovery stage included 25,822 subjects (2,181 ERP cases) from eight independent cohorts with

330   genetic and phenotypic data available for analyses: the British Genetics of Hypertension (BRIGHT)

331   study, the Gutenberg Health Study (GHS1, GHS2), the Genetic Regulation of Arterial Pressure In

332   humans in the Community (GRAPHIC) study, the Lifelines Cohort Study (Lifelines), the Study of

333   Health in Pomerania (SHIP, SHIP-Trend), and TwinsUK. Additional 13,634 subjects (1,124 ERP

334   cases) from four cohorts (Rotterdam Study I, II, III, and CHRIS) were used as independent replication:

335   the Rotterdam Study (Rotterdam Study I, II, III), and the Cooperative Health Research In South Tyrol

336   (CHRIS) study. The included subjects of all cohorts were of European ancestry, and all cohorts but

337   BRIGHT (which sampled hypertensive cases) were population based (**Supplementary Table 6**). The

338   determination of the discovery and replication cohorts was determined upfront based on the timeline of

339   the availability of the genetic and ERP data.

340   *Electrocardiogram analysis and ERP evaluation*

341   12-lead ECGs of all 12 studies were obtained during a study visit in a supine position after

342   approximately five minutes of rest and were analyzed manually by experienced and specifically trained

343   cardiologists for the presence of ERP. In detail, ECGs from TwinsUK and BRIGHT were evaluated in

344   the UK (YJ, RB, ERB), ECGs from all other cohorts were evaluated in Germany (TT, BK, CH, WR).

345   Paper-printed 12-lead ECGs were independently read by two experienced clinicians who were blinded

346   with respect to age and sex. There was very high level of agreement between each pair of interpreters

347   (95-98%)(20, 21). Cases of ambiguous or unequal phenotype were jointly reassessed by two readers,

348   and a consensus decision was achieved. To determine interobserver variability between UK and

349   German teams, a subset of ECGs was analyzed by both teams yielding a concordance of 96%(20,

350   21).

351   The ERP phenotype was established according to the definition by Haissaguerre and Macfarlane(6,

352   23). ERP was defined as elevation of the J-point above the level of QRS onset of ≥0.1 mV in at least

353   two corresponding leads. To avoid confusion or overlap with Brugada syndrome or arrhythmogenic

354   right ventricular dysplasia, leads V1 to V3 were excluded from ERP scoring. In case of presence of

355   ERP, region, either inferior (leads II, III, aVF), antero-lateral (leads I, aVL, V_4-V_6), or both, and the

356   maximum amplitude of J-point elevation was documented. Further, the morphology of ERP was

357   assessed as either notching, slurring or both as well as the ST segment according to Tikkanen and

358   collegues(44) as either concave/rapidly ascending (>0.1 mV elevation 100 ms after J-point peak or

359   persistently elevated ST segment >0.1 mV) or horizontal/descending (≤0.1 mV elevation within 100 ms

360   after J-point peak)(23, 44). In case of a QRS duration of >120 ms or rhythm other than sinus rhythm

361   (e.g. atrial fibrillation, pacemaker stimulation) ECGs were excluded from the analysis.

362   *Statistics*

363   Unless stated otherwise, the analyses were conducted and plotted using the R statistical software(46),

364   a Z-test was applied, and all reported p-values are two-sided.

365   *GWAS in individual studies*

366   The GWAS in each study for both the discovery and replication stage was performed on autosomal

367   imputed SNP genotypes using study-specific quality control protocols which are provided in detail in

368   **Supplementary Table 6**. Association analyses were performed using logistic regression for ERP

369   status as outcome and an additive genetic model on SNP dosages, thus taking genotype uncertainties

370   of imputed SNPs into account. The analyses were adjusted for age, sex, and relevant study-specific

371   covariates such as principal components for population stratification (**Supplementary Table 6**).

372   *Meta-analysis of individual study GWAS results*

373   The result files from individual studies GWAS underwent extensive quality control before meta-

374   analysis using the gwasqc() function of the GWAtoolbox package v2.2.4(47). The quality control

375   included file format checks as well as plausibility and distributions of association results including

376   effect sizes, standard errors, allele frequencies and imputation quality of the SNPs.

377   The meta-analyses were conducted using a fixed-effect inverse variance weighting as implemented in

378   Metal(48). Monomorphic SNPs, SNPs with implausible association results (i.e. p≤0, SE≤0,

379 |log(OR)|≥1000), and SNPs with an imputation quality score ≤0.4 were excluded prior to the meta-

380   analyses resulting in a median of 12,839,202 SNPs per cohort (IQR: 10,756,073-13,184,807). During

381   the meta-analysis, the study-specific results were corrected by their specific λ_{GC} if >1. Results were

382   checked for possible errors like use of incorrect association model by plotting the association p-values

383   of the analyses against those from a z-score based meta-analysis for verifying overall concordance.

384   SNPs that were present in <75% of the total sample size contributing to the respective meta-analysis

385   or with a MAF ≤0.01 were excluded from subsequent analyses. Finally, data for up to 6,976,246 SNPs

386   were available after the meta-analysis.

387   Quantile-quantile plots of the meta-analysis results are provided in **Supplementary Figure 2**. To

388   assess whether there was an inflation of p-values in the meta-analysis results attributed to reasons

389   other than polygenicity, we performed LD score regression(49). The LD score corrected λ_{GC} value of

390   the discovery and replication combined meta-analysis was 1.01, supporting the absence of

391   unaccounted population stratification. Genome-wide significance was defined as a p-value <5E-8,

392   corresponding to a Bonferroni correction of one million independent tests(50). The I^2 statistic was used

393   to evaluate between-study heterogeneity(51).

394   To evaluate the presence of allelic heterogeneity within each locus, the GCTA stepwise model

395   selection procedure (cojo-slct algorithm) was used to identify independent variants employing a step-

396   wise forward selection approach(52). We used the genotype information of 4,081 SHIP individuals for

397   LD estimation, and set the significance threshold for independent SNPs to 5E-8.

398   All loci were named according to the nearest gene of the lead SNP. Genomic positions correspond to

399   build 37 (GRCh37).

400   *Replication analysis*

401   To minimize the burden for multiple testing correction and thus maximizing the power for replication,

402   the lead SNPs of genome-wide significant loci in the discovery stage were taken forward to the

403   replication stage in independent samples (**Table 1**). SNPs were considered as replicated if the p-value

404   of a one-sided association test was <0.025 which corresponds to a Bonferroni correction for the two

405   lead SNPs tested at 5% significance level.

406   Finally, the GWAS results from the discovery and replication studies were meta-analyzed to search for

407   additional genome-wide significant loci by maximizing the statistical power for locus discovery.

408   *Gene expression based analyses*

409   The lead SNP rs1545300 of the *KCND3* locus of the combined discovery and replication GWAS meta-

410   analysis was tested for *cis* eQTLs (±1Mb window around the transcription start site) in 48 tissues

411   available in the GTEx v7 database that included at least 70 samples. Significant associations were

412   selected based on a Bonferroni corrected p-value <3.0E-5 for the number of genes and tissues tested.

413   Subsequently, the SNP rs1545300 was tested and plotted for co-localization in the three tissues with

414   an eQTL FDR<0.2 by applying the SMR method(53) using the GWAS and GTEx eQTL summary

415   statistics. The method includes a test whether the effect on expression observed at a SNP or at its

416   proxies is independent of the signal observed in the GWAS, i.e. that gene expression and y are

417   associated only because of a latent non-genetic confounding variable (SMR test), and a second test

418   that evaluates if the eQTL and GWAS associations can be attributable to the same causative variant

419   (HEIDI test). Significance for co-localization of the gene expression and the GWAS signals was

420   defined by $p_{SMR}<0.01$, where additionally a $p_{HEIDI}\geq0.05$ indicates the same underlying causal

421   variant(53).

422   *Data availability*

423   Summary association results of the combined GWAS meta-analysis have been submitted for full

424   download   to   the   CHARGE   dbGaP   website   under   accession   phs000930

425   [https://www.ncbi.nlm.nih.gov/gap].

426   *Study approval*

427   All subjects gave written informed consent and all participating studies were approved by the local

428   ethics committees and followed the recommendations of the Declaration of Helsinki.

429   **<u>Author Contributions</u>**

430   Project design and analysis: W.R., T.T., A.T., M.D, E.R.B. Management of individual study: A.F.D.,

431   C.F., C.P., E.R.B., K.J.L., M.A.I., M.D., M.G., M.Z., N.P., N.V., P.B.M., P.P., P.v.d.H., S.A., S.B.F.,

432   T.D.S., T.M., T.T., W.R., Y.J. Recruitment of individual study subjects: A.F.D., G.S., H.S., I.D., M.D.,

442 **References**

443 1. Reinhard W et al. The early repolarization pattern: Echocardiographic characteristics in elite
444 athletes. *Ann. Noninvasive Electrocardiol.* 2018;e12617.
445 2. Sinner MF et al. Association of early repolarization pattern on ECG with risk of cardiac and all-
446 cause mortality: a population-based prospective cohort study (MONICA/KORA). *PLoS Med.*
447 2010;7(7):e1000314.
448 3. Noseworthy PA et al. The early repolarization pattern in the general population: clinical correlates
449 and heritability. *J. Am. Coll. Cardiol.* 2011;57(22):2284–9.
450 4. Uberoi A et al. Early repolarization in an ambulatory clinical population. *Circulation*
451 2011;124(20):2208–14.
452 5. Trenkwalder T et al. Left ventricular geometry and function in early repolarization: results from the
453 population-based Gutenberg Health Study. *Clin. Res. Cardiol.* [published online ahead of print:
454 February 28, 2019]; doi:10.1007/s00392-019-01445-7
455 6. Haïssaguerre M et al. Sudden cardiac arrest associated with early repolarization. *N. Engl. J. Med.*
456 2008;358(19):2016–23.
457 7. Priori SG et al. HRS/EHRA/APHRS expert consensus statement on the diagnosis and management
458 of patients with inherited primary arrhythmia syndromes: document endorsed by HRS, EHRA, and
459 APHRS in May 2013 and by ACCF, AHA, PACES, and AEPC in June 2013. *Hear. Rhythm*
460 2013;10(12):1932–63.
461 8. Rosso R et al. J-point elevation in survivors of primary ventricular fibrillation and matched control
462 subjects: incidence and clinical significance. *J. Am. Coll. Cardiol.* 2008;52(15):1231–8.
463 9. Tikkanen JT et al. Long-term outcome associated with early repolarization on electrocardiography.
464 *N. Engl. J. Med.* 2009;361(26):2529–37.
465 10. Koncz I et al. Mechanisms underlying the development of the electrocardiographic and arrhythmic
466 manifestations of early repolarization syndrome. *J. Mol. Cell. Cardiol.* 2014;68:20–8.
467 11. Yan GX, Antzelevitch C. Cellular basis for the electrocardiographic J wave. *Circulation*
468 1996;93(2):372–9.
469 12. Haïssaguerre M et al. Ventricular fibrillation with prominent early repolarization associated with a
470 rare variant of KCNJ8/KATP channel. *J. Cardiovasc. Electrophysiol.* 2009;20(1):93–8.
471 13. Chauveau S et al. Early repolarization syndrome caused by de novo duplication of KCND3
472 detected by next-generation sequencing. *Hear. case reports* 2017;3(12):574–578.
473 14. Yao H et al. SCN1Bβ mutations that affect their association with Kv4.3 underlie early repolarization
474 syndrome. *J. Cell. Mol. Med.* 2018;22(11):5639–5647.
475 15. Liu X et al. A mutation in the CACNA1C gene leads to early repolarization syndrome with
476 incomplete penetrance: A Chinese family study. *PLoS One* 2017;12(5):e0177532.
477 16. Antzelevitch C et al. J-Wave syndromes expert consensus conference report: Emerging concepts
478 and gaps in knowledge.
479 17. Casado Arroyo R et al. Electrophysiological Basis for Early Repolarization Syndrome. *Front.*

480   *Cardiovasc. Med.* 2018;5:161.

481   18. Nunn LM et al. Prevalence of J-point elevation in sudden arrhythmic death syndrome families. *J.*
482   *Am. Coll. Cardiol.* 2011;58(3):286–90.

483   19. Mellor G et al. The Prevalence and Significance of the Early Repolarization Pattern in Sudden
484   Arrhythmic Death Syndrome Families. *Circ. Arrhythm. Electrophysiol.* 2016;9(6).
485   doi:10.1161/CIRCEP.116.003960

486   20. Reinhard W et al. Heritability of early repolarization: a population-based study. *Circ. Cardiovasc.*
487   *Genet.* 2011;4(2):134–8.

488   21. Bastiaenen R et al. The narrow-sense and common single nucleotide polymorphism heritability of
489   early repolarization. *Int. J. Cardiol.* [published online ahead of print: October 4, 2018];
490   doi:10.1016/j.ijcard.2018.09.119

491   22. Sinner MF et al. A meta-analysis of genome-wide association studies of the electrocardiographic
492   early repolarization pattern. *Hear. Rhythm* 2012;9(10):1627–34.

493   23. Macfarlane PW et al. The Early Repolarization Pattern: A Consensus Paper. *J. Am. Coll. Cardiol.*
494   2015;66(4):470–7.

495   24. GTEx Consortium et al. Genetic effects on gene expression across human tissues. *Nature*
496   2017;550(7675):204–213.

497   25. MacArthur J et al. The new NHGRI-EBI Catalog of published genome-wide association studies
498   (GWAS Catalog) *Nucleic Acids Res.* 2017;45(D1):D896–D901.

499   26. Christophersen IE et al. Fifteen Genetic Loci Associated With the Electrocardiographic P Wave.
500   *Circ. Cardiovasc. Genet.* 2017;10(4). doi:10.1161/CIRCGENETICS.116.001667

501   27. Roselli C et al. Multi-ethnic genome-wide association study for atrial fibrillation. *Nat. Genet.*
502   2018;50(9):1225–1233.

503   28. Nielsen JB et al. Biobank-driven genomic discovery yields new insight into atrial fibrillation biology.
504   *Nat. Genet.* 2018;50(9):1234–1239.

505   29. Verweij N et al. Genetic Determinants of P Wave Duration and PR Segment *Circ. Cardiovasc.*
506   *Genet.* 2014;7(4):475–481.

507   30. Verweij N et al. Twenty-eight genetic loci associated with ST-T-wave amplitudes of the
508   electrocardiogram. *Hum. Mol. Genet.* 2016;25(10):2093–2103.

509   31. Canela-Xandri O, Rawlik K, Tenesa A. An atlas of genetic associations in UK Biobank *Nat. Genet.*
510   2018;50(11):1593–1599.

511   32. Mercer BN et al. Early Repolarization Syndrome; Mechanistic Theories and Clinical Correlates.
512   *Front. Physiol.* 2016;7:266.

513   33. Haïssaguerre M et al. Characteristics of recurrent ventricular fibrillation associated with
514   inferolateral early repolarization role of drug therapy. *J. Am. Coll. Cardiol.* 2009;53(7):612–9.

515   34. Mavragani-Tsipidou P, Scouras ZG, Haralampidis K, Lavrentiadou S, Kastritsis CD. The polytene
516   chromosomes of Drosophila triauraria and D. quadraria, sibling species of D. auraria. *Genome*
517   1992;35(2):318–26.

518   35. Haïssaguerre M et al. Depolarization versus repolarization abnormality underlying inferolateral J-
519   wave syndromes: New concepts in sudden cardiac death with apparently normal hearts. *Hear.*
520   *Rhythm* [published online ahead of print: November 2, 2018]; doi:10.1016/j.hrthm.2018.10.040

521   36. Bonasio R, Shiekhattar R. Regulation of transcription by long noncoding RNAs. *Annu. Rev. Genet.*
522   2014;48(1):433–55.

523   37. Ulitsky I. Evolution to the rescue: using comparative genomics to understand long non-coding
524   RNAs. *Nat. Rev. Genet.* 2016;17(10):601–14.

525   38. Sallam T, Sandhu J, Tontonoz P. Long Noncoding RNA Discovery in Cardiovascular Disease:
526   Decoding Form to Function. *Circ. Res.* 2018;122(1):155–166.

527   39. Harismendy O et al. 9p21 DNA variants associated with coronary artery disease impair interferon-
528   γ signalling response. *Nature* 2011;470(7333):264–8.

529   40. Broadbent HM et al. Susceptibility to coronary artery disease and diabetes is encoded by distinct,
530   tightly linked SNPs in the ANRIL locus on chromosome 9p. *Hum. Mol. Genet.* 2008;17(6):806–14.

531   41. Medeiros-Domingo A et al. Gain-of-function mutation S422L in the KCNJ8-encoded cardiac
532   K(ATP) channel Kir6.1 as a pathogenic substrate for J-wave syndromes. *Hear. Rhythm*
533   2010;7(10):1466–71.

534   42. Barajas-Martínez H et al. Molecular genetic and functional association of Brugada and early
535   repolarization syndromes with S422L missense mutation in KCNJ8 *Hear. Rhythm* 2012;9(4):548–555.

536   43. Landrum MJ et al. ClinVar: public archive of interpretations of clinically relevant variants. *Nucleic*
537   *Acids Res.* 2016;44(D1):D862-8.

538   44. Tikkanen JT et al. Early repolarization: electrocardiographic phenotypes associated with favorable
539   long-term outcome. *Circulation* 2011;123(23):2666–73.

540   45. Cheng Y-J et al. Role of Early Repolarization Pattern in Increasing Risk of Death. *J. Am. Heart*

541 *Assoc.* 2016;5(9). doi:10.1161/JAHA.116.003375

542 46. R Development Core Team, R Core Team. R: A Language and Environment for Statistical
543 Computing [Internet]2016;https://www.r-project.org. cited April 2, 2016

544 47. Fuchsberger C, Taliun D, Pramstaller PP, Pattaro C, CKDGen consortium. GWAtoolbox: an R
545 package for fast quality control and handling of genome-wide association studies meta-analysis data.
546 *Bioinformatics* 2012;28(3):444–445.

547 48. Willer CJ, Li Y, Abecasis GR. METAL: fast and efficient meta-analysis of genomewide association
548 scans. *Bioinformatics* 2010;26(17):2190–1.

549 49. Bulik-Sullivan BK et al. LD Score regression distinguishes confounding from polygenicity in
550 genome-wide association studies. *Nat. Genet.* 2015;47(3):291–5.

551 50. Pe'er I, Yelensky R, Altshuler D, Daly MJ. Estimation of the multiple testing burden for
552 genomewide association studies of nearly all common variants. *Genet Epidemiol* 2008;32(4):381–385.

553 51. Higgins JPT, Thompson SG, Deeks JJ, Altman DG. Measuring inconsistency in meta-analyses.
554 *BMJ* 2003;327(7414):557–560.

555 52. Yang J, Lee SH, Goddard ME, Visscher PM. GCTA: a tool for genome-wide complex trait analysis.
556 *Am. J. Hum. Genet.* 2011;88(1):76–82.

557 53. Zhu Z et al. Integration of summary data from GWAS and eQTL studies predicts complex trait
558 gene targets. *Nat. Genet.* 2016;48(5):481–7.

559 54. Pruim RJ et al. LocusZoom: regional visualization of genome-wide association scan results.
560 *Bioinformatics* 2010;26(18):2336–7.

561 55. Dreszer TR et al. The UCSC Genome Browser database: extensions and updates 2011. *Nucleic
562 Acids Res* 2012;40(Database issue):D918--D923.

563

Figure Legends

565   **Figure 1. GWAS results of the *KCND3* locus**

566   The results of the combined early repolarization pattern (ERP) GWAS results for the *KCND3* locus are

567   shown for the replicated discovery stage lead SNP rs12090194 in n=38,811 individuals (A and B), and

568   for the combined GWAS lead SNP rs1545300 in n=38,806 individuals (C and D). The regional

569   association plots (A and C) show the association results in a ±500 kb region around the lead SNP.

570   SNPs are plotted on the x-axis according to their chromosomal position with the $-\log_{10}$(p-value) of the

571   GWAS association on the y-axis. Correlation with the lead SNP (purple) is estimated based on the

572   1000 Genomes reference samples. Plots were generated using the website of LocusZoom[54].

573   Genetic positions refer to GRCh37/hg19 coordinates. Forest plots of the respective lead SNPs are

574   provided in (B) and (D), with odds ratios and their 95% confidence intervals plotted on the x-axis. I² is

575   the percentage of total variation across studies that is due to heterogeneity.

576   **Figure 2. Location of the significantly associated SNPs within the *KCND3* gene**

577   The top 43 SNPs with a genome-wide significance visualized by UCSC Genome Browser[55]. All

578   SNPs mapped into *KCND3* gene. The two leads SNPs rs1545300 and rs12090194 of the discovery

579   and combined meta-analyses are reported with a red and an orange diamond, respectively. The

580   H3K27Ac mark track (Layered H3K27Ac) shows the levels of enrichment of the H3K27Ac histone

581   mark. Chemical modifications (e.g. methylation and acylation) to the histone proteins present in

582   chromatin influence gene expression by changing how accessible the chromatin is to transcription.

583   The H3K27Ac histone mark is thought to enhance transcription possibly by blocking the spread of the

584   repressive histone mark H3K27Me3. The GeneHancer (GH) track set shows human regulatory

585   elements, i.e. enhancers (gray) and promoters (red), containing tracks representing regulatory

586   elements (Reg Elems), gene transcription start sites (TSS), associations between regulatory elements

587   and genes (Interactions), and clustered interactions (Clusters). A gray box in the DNaseI

588   Hypersensitivity Clusters track (DNase Clusters) indicates the extent of the hypersensitive region with

589   darkness proportional to the maximum signal strength observed in any cell line. A gray box in the

590   Transcription Factor ChIP-seq Clusters track (Txn Factor ChIP) indicates a cluster of transcription

591   factor occupancy, with the darkness of the box being proportional to the maximum signal strength

592   observed in any cell line contributing to the cluster.

Figure 3. Co-localization results

Illustration of the SMR test for the early repolarization pattern (ERP) risk and the expression quantitative trait loci (eQTLs) at the rs1545300 locus at chromosome 1p13.2 for (A) left ventricle of the heart, (B) tibial artery, and (C) minor salivary gland tissue. The sample size for the eQTLs are n=272, n=388 and n=85 in panels (A), (B) and (C), respectively. In each panel, the upper box shows the GWAS regional association plot with ERP risk of the combined GWAS (n=39,456), with level of significance of the SMR test (y-axis) for each transcript in the locus indicated by a diamond positioned at the center of the transcript. A significant SMR test represented by a purple diamond indicates an association of the transcript level of the respective genes (purple label) with the trait. For all three tissues, an increased gene expression level of a significant SMR test was associated with a higher risk of ERP. A filled purple diamond indicates a HEIDI test p-value >0.05, thus a likely co-localization. The lower box shows the regional association distribution with changes in expression of the highlighted (purple) gene transcript in the respective tissue. In both boxes, the x-axis refers to GRCh37/hg19 genomic coordinates.

608 **Table 1: Baseline characteristics of the study populations**

Study	Subgroup	Number of samples (n)	Number of females (n)	Age in years (mean±SD)	Heart rate in bpm (mean±SD)	BMI (mean±SD)
Discovery stage						
BRIGHT	ERP+	189	105	57.6±12.1	61.7±9.9	27.7±3.4
	ERP-	1173	747	59.4±12.3	63.7±11.2	27.4±3.8
GHS1	ERP+	182	60	54.5±10.0	67.6±11.5	26.8±4.4
	ERP-	2628	1358	55.6±10.9	69.1±10.8	27.1±4.7
GHS2	ERP+	70	26	54.0±10.2	67.1±11.4	27.5±5.5
	ERP-	1028	536	54.9±10.9	68.7±10.8	27.2±4.9
GRAPHIC	ERP+	57	18	52.3±3.9	63.5±8.0	27.4±4.0
	ERP-	893	457	52.8±4.5	64.1±9.8	27.4±4.3
Lifelines	ERP+	1253	639	48.0±11.5	66.3±10.9	25.7±3.8
	ERP-	11463	6902	47.9±11.3	68.4±11.5	26.4±4.3
SHIP	ERP+	173	79	46.6±16.1	70.5±11.6	25.9±4.2
	ERP-	2835	1508	48.5±15.8	73.7±11.6	27.3±4.9
SHIP-Trend	ERP+	86	38	49.8±14.5	64.4±8.9	26.9±4.4
	ERP-	848	494	49.7±13.4	65.9±9.6	27.3±4.6
TwinsUK	ERP+	171	150	51.7±13.2	64.1±10.3	25.3±4.4
	ERP-	2773	2651	52.7±12.4	66.8±10.4	25.7±4.6
Replication stage						
CHRIS	ERP+	427	159	45.2±16.3	60.3±8.9	25.4±4.2
	ERP-	3953	2318	45.7±16.1	62.5±8.8	25.6±4.6
Rotterdam Study I	ERP+	308	182	66.4±7.6	68.7±11.6	27.5±7.4
	ERP-	4438	2739	66.3±7.7	69.2±11.9	27.1±6.9
Rotterdam Study II	ERP+	164	84	64.1±7.3	67.5±10.6	27.5±4.1
	ERP-	1476	825	64.4±7.5	68.8±10.8	27.5±4.1
Rotterdam Study III	ERP+	225	116	56.7±5.6	69.0±11.7	27.6±4.9
	ERP-	2643	1541	57.0±6.7	69.6±10.5	27.5±5.0

609
610 ERP+: cases with early repolarization pattern; ERP-: controls

611 **Table 2: Lead SNPs of the GWAS association results**

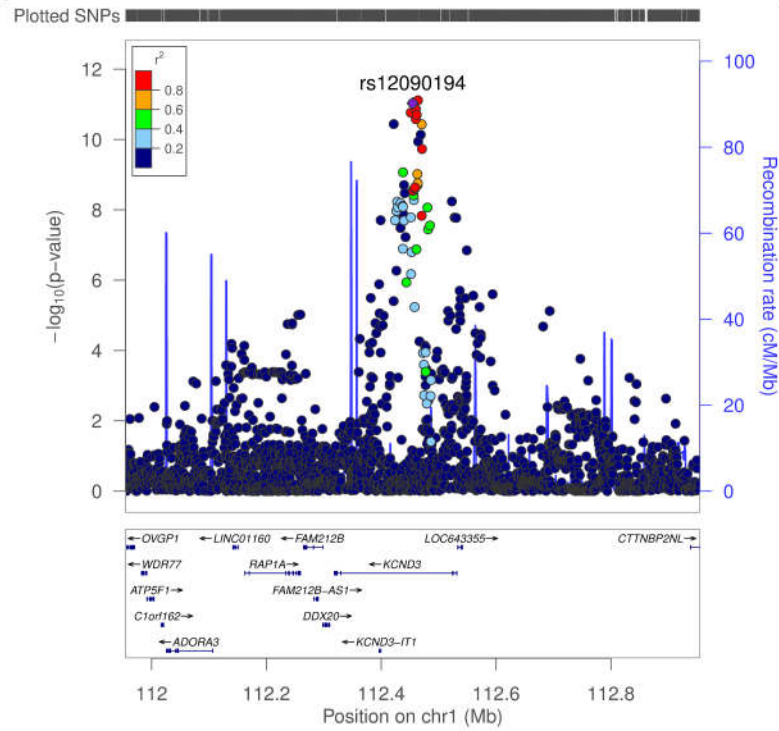| SNP	Chr:position	A1/ A2	Nearest gene	AF1	Discovery OR	P	I²	N	Replication OR	P	I²	N	Combined OR	P	I²	N
rs12090194	1:112,454,822	t/c	*KCND3*	0.32	0.80 [0.75-0.86]	**4.6E-10**	34	25177	0.86 [0.79-0.95]	2.5E-03	39	13634	0.82 [0.78-0.87]	9.3E-12	35	38811
rs1545300	1:112,464,004	t/c	*KCND3*	0.32	0.81 [0.75-0.86]	1.4E-09	41	25172	0.85 [0.77-0.94]	9.4E-04	56	13634	0.82 [0.78-0.87]	**7.7E-12**	43	38806
rs139772527	16:208,761	t/c	*HBZ*	0.01	2.57 [1.85-3.58]	**2.0E-08**	0	21495	1.21 [0.85-1.73]	2.8E-01	0	13634	1.81 [1.42-2.31]	1.4E-06	11	35129

612
613 A1: effect allele; AF1: allele frequency of A1; Chr: chromosome; position: position corresponding to
614 build 37 (GRCh37); OR: odds ratio of A1 [95% confidence interval]; P: association p-value; I²:
615 percentage of total variation across studies that is due to heterogeneity; N: sample size. Bold values
616 indicate the lead SNP (lowest p-value) of a significantly associated locus in the corresponding meta-
617 analysis stage.
618

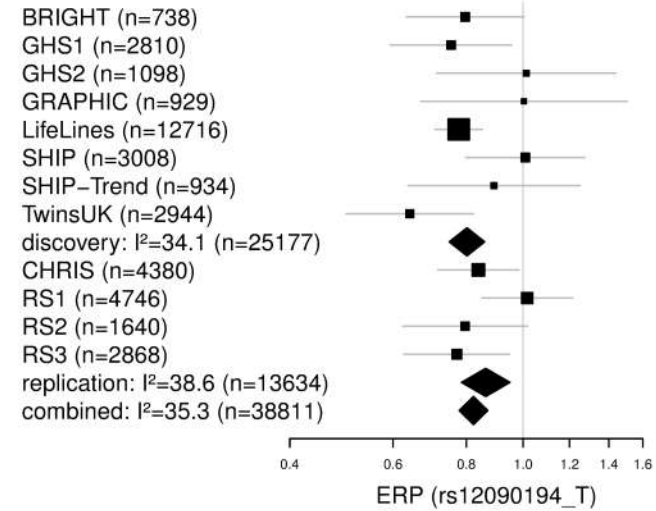**Table 3: The 43 genome-wide significant SNPs of the *KCND3* locus**

SNP	position	location	A1/A2	AF1	OR	P
rs817972	112,399,057	intron	a/g	0.90	1.35 [1.22-1.50]	2.0E-08
rs583731	112,421,854	intron	t/c	0.09	0.69 [0.62-0.77]	3.6E-11
rs528779	112,424,077	intron	t/c	0.71	1.18 [1.11-1.25]	2.0E-08
rs612790	112,426,577	intron	c/g	0.29	0.84 [0.80-0.89]	1.1E-08
rs2813862	112,427,918	intron	c/g	0.29	0.84 [0.79-0.89]	5.9E-09
rs1767283	112,428,953	intron	t/c	0.29	0.84 [0.80-0.89]	8.5E-09
rs11102354	112,433,666	intron	a/g	0.31	1.18 [1.11-1.25]	3.3E-08
rs605604	112,433,863	intron	a/c	0.70	1.19 [1.12-1.26]	6.4E-09
rs2798334	112,437,344	intron	t/c	0.30	0.84 [0.79-0.89]	7.7E-09
rs2813864	112,437,853	intron	a/g	0.29	0.84 [0.79-0.89]	8.2E-09
rs2587368	112,437,907	intron	t/c	0.40	0.86 [0.81-0.90]	1.7E-08
rs2813865	112,437,956	intron	a/g	0.25	0.82 [0.77-0.87]	8.6E-10
rs894849	112,437,964	intron	t/c	0.41	0.86 [0.81-0.90]	1.3E-08
rs608673	112,439,757	intron	t/c	0.44	0.86 [0.81-0.91]	2.0E-08
rs7539683	112,439,770	intron	t/g	0.27	1.20 [1.13-1.27]	2.0E-09
rs1805222	112,440,983	intron	a/g	0.27	1.20 [1.13-1.27]	3.3E-09
rs2120436	112,451,447	intron	t/c	0.32	0.82 [0.78-0.87]	1.7E-11
rs2034124	112,451,681	intron	a/g	0.45	1.16 [1.10-1.22]	1.6E-08
rs12090194	112,454,822	intron	t/c	0.32	0.82 [0.78-0.87]	9.3E-12
rs72692596	112,455,415	intron	t/c	0.32	0.84 [0.79-0.89]	2.8E-09
rs72692597	112,455,442	intron	t/g	0.32	0.84 [0.79-0.89]	2.9E-09
rs4839182	112,456,538	intron	a/g	0.55	1.18 [1.12-1.25]	3.9E-09
rs4839183	112,456,882	intron	a/g	0.46	1.17 [1.11-1.23]	5.3E-09
rs72692602	112,458,833	intron	t/c	0.68	1.20 [1.13-1.27]	2.5E-09
rs72694603	112,458,893	intron	t/c	0.32	0.83 [0.79-0.89]	2.3E-09
rs4839184	112,460,221	intron	c/g	0.32	0.83 [0.78-0.87]	2.6E-11
rs4839185	112,460,262	intron	t/c	0.68	1.21 [1.15-1.28]	1.4E-11
rs1443926	112,461,902	intron	a/g	0.68	1.21 [1.15-1.28]	2.0E-11
rs6682872	112,462,984	intron	a/g	0.60	1.18 [1.12-1.24]	9.6E-10
rs4838926	112,463,323	intron	c/g	0.40	0.85 [0.81-0.90]	2.0E-09
rs4838927	112,463,617	intron	t/c	0.60	1.18 [1.12-1.24]	1.7E-09
rs1545300	112,464,004	intron	t/c	0.32	0.82 [0.78-0.87]	7.7E-12
rs17029069	112,464,376	intron	t/c	0.30	1.21 [1.14-1.28]	1.1E-10
rs12119724	112,468,814	intron	t/c	0.29	1.21 [1.14-1.28]	7.3E-11
rs11588747	112,470,474	intron	t/c	0.70	1.19 [1.12-1.27]	1.5E-08
rs2010749	112,470,581	intron	t/c	0.63	1.20 [1.14-1.27]	3.7E-11
rs1443927	112,471,029	intron	c/g	0.69	1.20 [1.14-1.28]	1.9E-10
rs12145374	112,480,536	intron	a/c	0.80	1.22 [1.14-1.30]	8.6E-09
rs72694622	112,481,667	intron	t/c	0.18	0.81 [0.75-0.87]	3.6E-08
rs12144965	112,484,962	intron	t/c	0.82	1.23 [1.14-1.32]	2.8E-08
rs3008527	112,523,095	intron	t/c	0.70	1.19 [1.12-1.26]	5.8E-09
rs3008528	112,527,869	intron	a/t	0.70	1.18 [1.11-1.25]	1.7E-08
rs2075811	112,530,626	intron	c/g	0.30	0.85 [0.80-0.90]	1.7E-08

621   A1: effect allele; AF1: allele frequency of A1; position on chromosome 1 (build 37, GRCh37); OR:
622   odds ratio of A1 [95% confidence interval]; P: association p-value. The SNPs are ordered by their
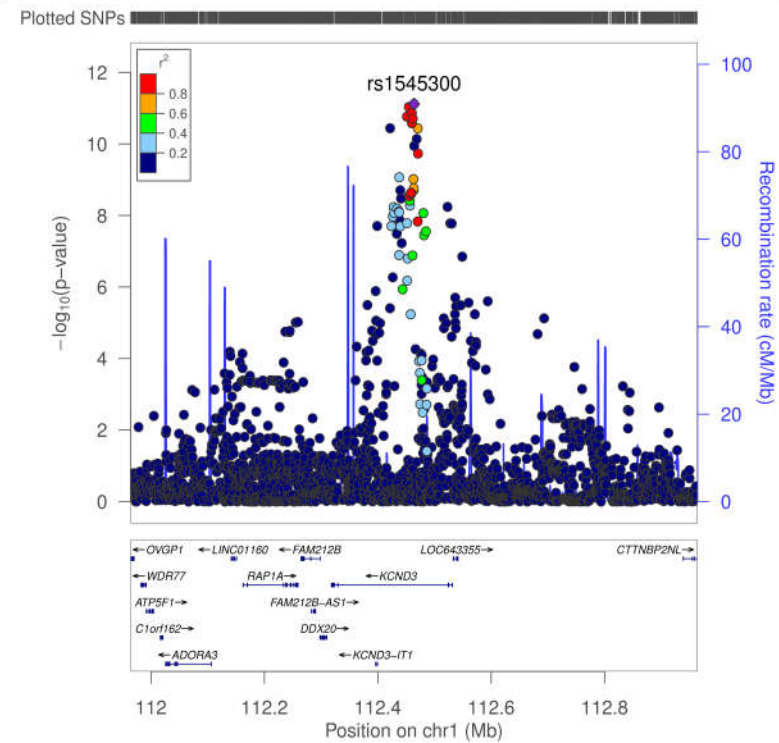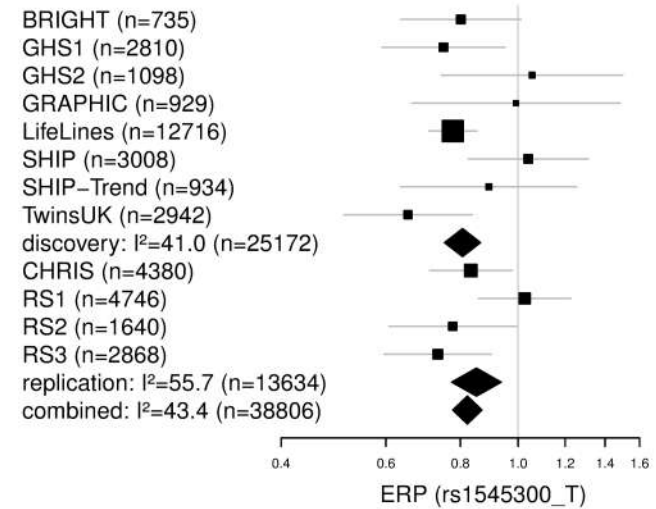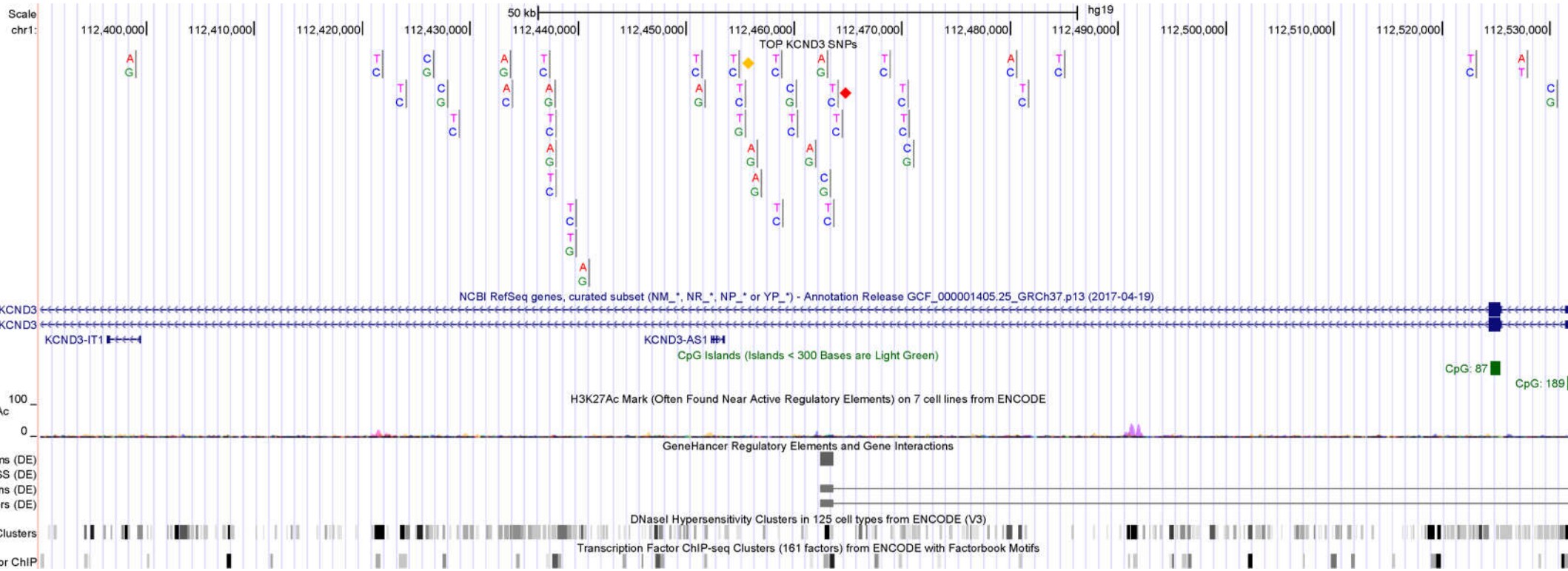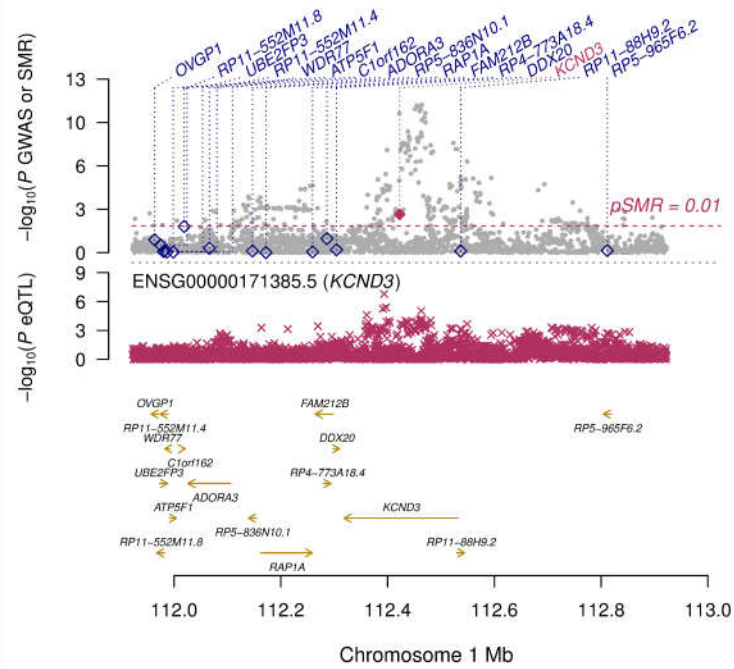623   position, and the results of the combined meta-analysis are given.